Publishing House
AKAPIT

COMPUTER METHODS IN MATERIALS SCIENCE

Informatyka w Technologii Materiałów

Vol. 8, 2008, No. 1

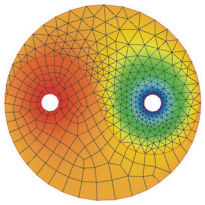

NUMERICAL MODELING OF INFLUENCE OF GASEOUS BUBBLE SHAPE FACTOR ON STEEL FLOW IN THE TUNDISH WITH SYSTEM OF ARGON INJECTION

ADAM CWUDZIŃSKI, JAN JOWSA

Department of Metals Extraction and Recirculation, Faculty of Materials Processing Technology and Applied Physics, Czestochowa University of Technology, Armii Krajowej 19, 42-200 Czestochowa, Poland
Corresponding Author: cwudzinski@mim.pcz.czest.pl (A. Cwudziński)

Abstract

The article presents the results of computer simulations of steel flow in a six-strand tundish with subflux controller of turbulence and system of argon injection. The authors employed the CFD (Computational Fluid Dynamics) numerical modeling technique to demonstrate the effect of different variants of gaseous bubble shape (spherical and nonspherical bubbles) on the steel flow in the zone of argon injection and shape of RTD (Residence Time Distribution) curves. The computer simulations were performed for isothermal conditions. As a result of computations, fields of steel flow, fields of turbulence intensity, RTD curves and the percentage shares of particular flow zones (stagnant flow, plug flow, and ideal mixing flow) were obtained.

Key words: numerical modeling, tundish, steel flow, system of argon injection, RTD curves, bubble shape factor

1. INTRODUCTION

The term "Argon steel metallurgy" (Anioła-Kusiak at al. 1981) means the use of argon for the production of steel of enhanced quality, because argon is excellently suitable for the chemical and thermal homogenization of steel and intensifies the flotation of non-metallic inclusions out of the steel to the slag phase. Argon is applied as early as on the stage of producing steel in converters of AOD (Argon-Oxygen-Decarburization) and TBM (Thyssen-Blast-Metallurgie) types. The work developed by (Stolte 2002) describes processes conducted in steelmaking ladles of RH (Recirculation Degasser) and REDA (Revolution Degassing Activator), VD (Tank Degasser), LF (Ladle Furnace) types, in which argon has been applied. In the works developed by Guy at al. (1991) and Moravec and Valek (2004), argon was applied during the continuous steel casting process in a tundish. Argon is also used for the protection of the steel surface against the action of air during the steel flow from the steelmaking ladle to the tundish and from the tundish to the casting mould in devices such as a shroud tube and sub-entry-nozzles (Rzeszowski at al. 2003). Research works have increasingly often been conducted recently, which deal with the application of argon in the tundish. The application of an inert gas injection system in the tundish involves the development of an appropriate steel argoning technology. The argon injection system must be adapted to the tundish design and used in accordance with the production schedule of the metallurgical works. Being usually expensive and interfering with the steelworks operational schedule, industrial pilot tests are being replaced with simulation studies (Cwudziński

ISSN 1641-8581

and Jowsa 2006, Pieprzyca at al. 2006, Moravec at al. 2005, Morales at al. 2004). The numerical code used for the studies enables the simulation of injection of constant-diameter gas bubbles. This is a considerable simplification, as the literature dealing with gas bubble motion describes phenomena, such as the disintegration and combination of bubbles, depending on the bubble position in the medium under study, the effect of gas injection intensity, variation in pressure and the temperature of the continuous medium (Anagbo and Brimacombe 1990, Iguchi M. at al. 1992a, Iguchi M. at al. 1992b, Zhou and Brimacombe 1994, Sheng and Irons 1995, Iguchi M. at al. 1995, Tatsuoka at al. 1997, Yokoya at al. 2000). The aforementioned phenomena lead to a change in the diameter and shape of the gas bubble. This work presents investigation results concerning the injection of gas bubbles of a non- and spherical shape. The effect of variation in the bubble shape on the motion of steel in the gas injection zone has been determined and RTD curves characterizing the hydrodynamic state of the facility investigated have been plotted. The calculations that have been made will serve for the assessment of to what extent the changes introduced to the numerical model will influence the obtained results and enable the development of a model that most accurately reflects the process of argon injection to the tundish.

2. CHARACTERIZATION OF THE TEST FACILITY AND TESTING METHODOLOGY

The subject of simulation was a six-strand tundish equipped with a subflux controller of turbulence (SCT) and four porous plugs. A SCT-type device was mounted in the tundish pouring zone and porous plugs between particular tundish outlets, as shown in Figure 1. A figure 2 and 3 shows detailed dimensions of the tundish and subflux controller of turbulence. Diameter of tundish outlet equals 17 millimetres. While width of porous plug equal 50 millimetres. The numerical simulation of the flow of steel and neutral gas was performed for half of the facility by generating a computational grid with the "symmetry" boundary condition extending through the tundish pouring zone, as shown in Figure 1.

The program Fluent was used for numerical simulation of steel flow. In this numerical code movement of continuous phase and discrete phase is describe by Euler-Lagrange approach. The continuous phase is treated as a continuum by solving the time averaged Navier-Stokes equations, while the dispersed phase is solved by tracking of bubbles through the calculated flow field (Discrete Phase Model). The system equations are as follows:

$$\frac{\partial \rho}{\partial t} + \nabla \cdot (\rho u) = 0 \tag{1}$$

$$\frac{\partial}{\partial t} \cdot (\rho u) + \nabla \cdot (\rho u u) = -\nabla p + \nabla \cdot (\overline{\overline{\tau}}) + \rho g \tag{2}$$

$$\overline{\overline{\tau}} = \mu \left[(\nabla u + \nabla u) - \frac{2}{3} \nabla \cdot u I \right] \tag{3}$$

where: $\overline{\overline{\tau}}$ - stress tensor (Pa), t – time [s], u – velocity [m/s], p – pressure [Pa], ρ – density [kg/m^3], g – gravitational acceleration [m/s^2], μ – viscosity [kg/m·s], I – unit tensor.

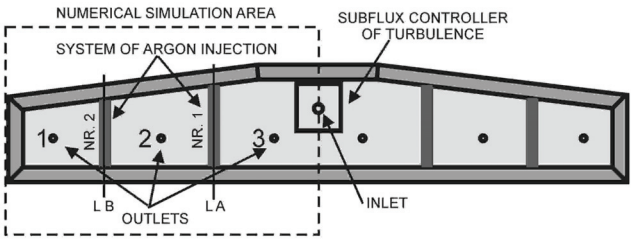

Fig. 1. Pictorial diagram of the tundish and position of the flow control devices

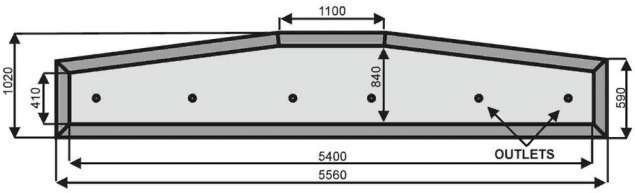

Fig. 2. Dimensions of the tundish

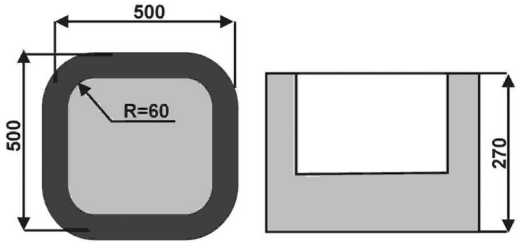

Fig. 3. Dimensions of the subflux controller of turbulence

For the description of the turbulence of steel flow through the tundish, the k-ε turbulence model was adopted, whose semi-empirical constants take on the following values: C_1= 1.44, C_2=1.92, σ_k=1.0, σ_ε= 1.3. The basic equations of the k-ε model describing are as follows:

$$\mu_t = \frac{C_\mu \rho k^2}{\varepsilon} \tag{4}$$

$$\frac{\partial \rho k}{\partial t} + \frac{\partial \rho u_i k}{\partial x_i} = \frac{\partial}{\partial x_i}\left(\frac{\mu_t}{\sigma_k}\frac{\partial k}{\partial x_i}\right) + G_k - \rho\varepsilon \tag{5}$$

$$\frac{\partial \rho \varepsilon}{\partial t} + \frac{\partial \rho u_i \varepsilon}{\partial x_i} = \frac{\partial}{\partial x_i}\left(\frac{\mu_t}{\sigma_\varepsilon}\frac{\partial \varepsilon}{\partial x_i}\right) + C_1\frac{\varepsilon}{k}G_k - C_2\frac{\varepsilon^2}{k} \tag{6}$$

$$G_k = \mu_t\left(\frac{\partial u_i}{\partial x_j} + \frac{\partial u_j}{\partial x_i}\right)\frac{\partial u_i}{\partial x_j} \tag{7}$$

where: C_μ - model constant 0.09, μ_t – dynamic turbulent viscosity [kg/m·s], k – kinetic energy of turbulence [m^2/s^2], ε – dissipation rate of turbulent kinetic [m^2/s^3], x_i – cartesian coordinate, G_k – generation of turbulent kinetic energy.

The boundary condition for the determinations of RTD curves was the impulse increase in tracer concentration at the tundish inlet at the time t=0, having the features of the Dirac function.

Physical quantities of liquid steel and argon were as follows: ρ_S – 7010 kg/m^3, μ_S – 0.007 kg/m·s, ρ_A – 1.62 kg/m^3. At the inlet tundish, liquid steel inflow of 2.5 m/s was assumed with turbulence intensity of 5 percent. For simulation of movement of gas phase Discrete Phase Model was used. This model is describing as follows:

$$\frac{du_B}{dt} = F_D(u - u_B) + \frac{g(\rho_B - \rho)}{\rho_B} \tag{8}$$

$$F_D = \frac{18\mu}{\rho_B d_B^2} + \frac{C_D \,\mathrm{Re}}{24} \tag{9}$$

$$\mathrm{Re} = \frac{\rho d_B |\underline{u} - \underline{u}_B|}{\mu} \tag{10}$$

$$C_D = \frac{24}{\mathrm{Re}}(1 + b_1 \mathrm{Re}^{b_2}) + \frac{b_3 \,\mathrm{Re}}{b_4 + \mathrm{Re}} \tag{11}$$

$$b_1 = \exp(2.3288 - 6.4581\phi + 2.4486\phi^2) \tag{12}$$

$$b_2 = 0.0964 + 0.5565\phi \tag{13}$$

$$b_3 = \exp(4.095 - 13.8944\phi + 18.4222\phi^2 - 10.2599\phi^3) \tag{14}$$

$$b_4 = \exp(1.4681 + 12.2584\phi - 20.7322\phi^2 + 15.8855\phi^3) \tag{15}$$

where: ρ – density of steel [kg/m^3], ρ_B – density of bubble [kg/m^3], μ – viscosity of steel [kg/m·s], u – velocity of steel, u_B – velocity of bubble, F_D - drag force of bubble [N], g – gravitational acceleration [m/s^2], d_B – diameter of bubble [m], Re – Reynolds number [-], C_D – drag coefficient [-], $b_1 \div b_4$ – parameters in the non-spherical bubble drag model.

The effects of the chaotic behavior of bubble during volume of steel movement are described by the discrete random walk model (DRW), also called the stochastic model, in which the local components of bubble velocity is proportional to the local effective energy of turbulence:

$$u_B' = \zeta\sqrt{\frac{2k}{3}} \tag{16}$$

where: u_B' – random velocity fluctuation [m/s], k – kinetic energy of turbulence [m^2/s^2], ζ – random number [-].

The injection of a neutral gas (argon) to the tundish filled with liquid steel was modelled. Gas was blown in through each of the porous plugs at a flow rate of 10 Nl/min. Simulations were performed for three variants of the gas bubble shape. In the first variant, the injection of 15 mm-diameter spherical bubbles was simulated. Since, according to (Iguchi at al. 1997), it can be assumed that the relationship between the average bubble diameter and the length of the ellipsoid chord in liquid iron is:

$$\bar{d}_B = 1.5\,\bar{L}_B \tag{17}$$

where: $\bar{d}_B$ – mean bubble diameter [m], $\bar{L}_B$ – mean bubble chord length [m].

So, in the remaining computation variants, bubbles had a non-spherical shape defined by the shape factor described by (Haider and Levenspiel 1989) and expressed by the following relationship:

$$\phi = \frac{s}{S} \tag{18}$$

where: s - surface of sphere having the same volume as the particle, S – actual surface area of the particle.

The shape coefficient for the simulated 15 mm-diameter bubbles was assumed to be at a level of 0.8 for variant 2 and 0.6 for variant 3. The different variants of the injected bubble shape, assumed in this work, are based on the work of (Szekely and Themelis 1971), where the authors have shown that the shape of gas bubbles is not ideally spherical, in particular where their diameter is greater than 4 mm.

3. COMPUTATION RESULTS

As a result of performed numerical computations, fields of steel flow and fields of turbulence intensity in the zones of neutral gas injection to the tundish were obtained. The numerical results of steel flow and turbulence intensity are presented for the gas bubble shape variants under consideration. Figures 4, 8 and 12 represent the motion of steel in the zone of interaction of porous plug no. 1 (the line A, Fig. 1), whereas figures 6, 10 and 14 - in the zone of interaction of porous plug no. 2 (the line B, Fig. 1). When assessing the effect of gas bubble shape variations on the formation of the vectorial velocity field it can be stated that the effect is scarcely visible in the zone of interaction of porous plug no. 1, in contrast to Zone B, where clear differences have shown up. One of the most important differences is the appearance of a distinct steel vortex in the free surface region. Figures 5, 7, 9, 11, 13 and 15 present the distribution of steel velocity along the characteristic measurement lines crossing the argon injection zones (L1, L2 and L3). The lines passed perpendicularly to the porous plug extend from the plug surface to the free steel table surface. The lines are positioned in the centre (L2) and on either side of the porous plug (L1 & L3). When analyzing the velocity of steel in the region of porous plug no. 1 for spherical bubbles (Fig. 5) we can see that the steel velocity is not distributed symmetrically and is distinctly greater on one of the tundish sides (L1). It has been noticed that the asymmetry of steel velocity distribution in the gas plug zone becomes disturbed for

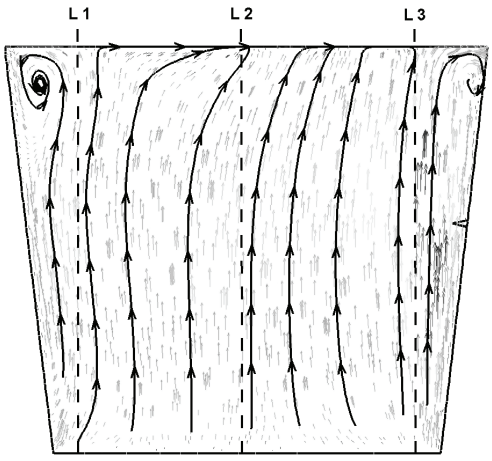

Fig. 4. Steel flow in the zone of Ar injection through blow shape number 1(spherical shape of bubble)

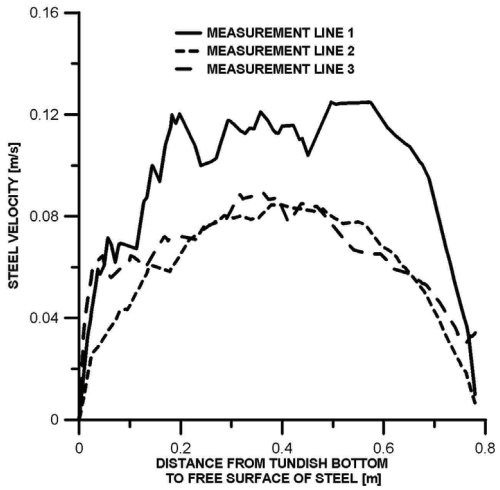

Fig. 5. Steel velocity along measurement line in the zone of Ar injection through blow shape number 1 (spherical shape of bubble)

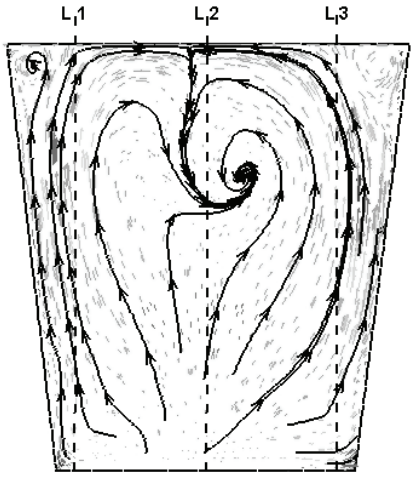

Fig. 6. Steel flow in the zone of Ar injection through blow shape number 2 (spherical shape of bubble)

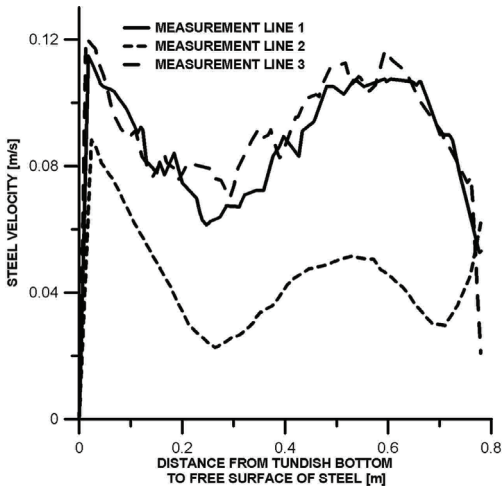

Fig. 7. Steel velocity along measurement line in the zone of Ar injection through blow shape number 2 (spherical shape of bubble)

non-spherical bubbles (the bubble shape factor = 0.8, Fig. 9) and this state aggravates in the case of the

flow of bubbles defined by the shape factor equal to 0.6 (Figs. 13 & 15).

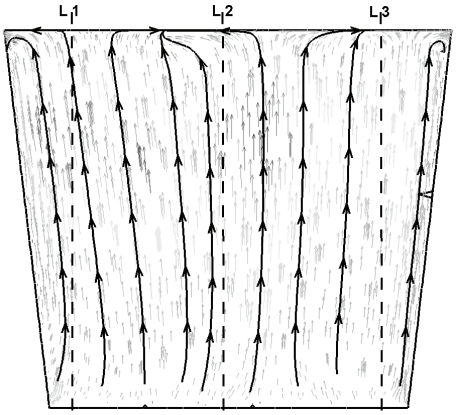

Fig. 8. Steel flow in the zone of Ar injection through blow shape number 1 (shape factor of bubble = 0.8)

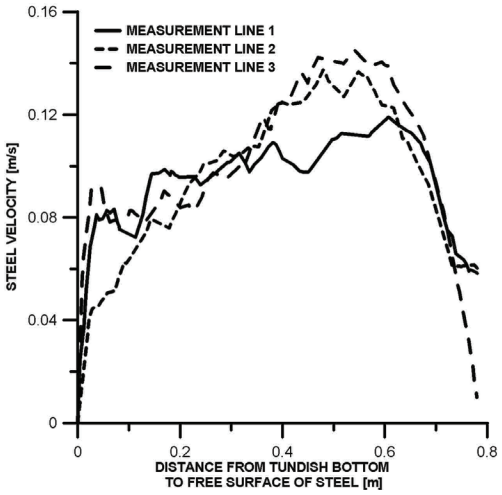

Fig. 9. Steel velocity along measurement line in the zone of Ar injection through blow shape number 1 (shape factor of bubble = 0.8)

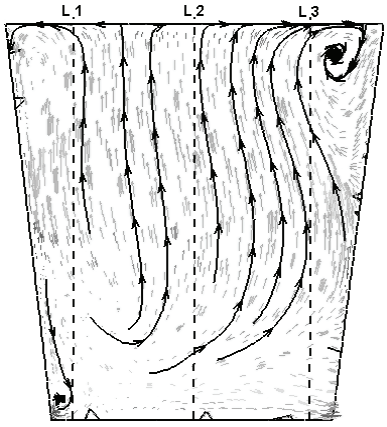

Fig. 10. Steel flow in the zone of Ar injection through blow shape number 2 (shape factor of bubble = 0.8)

Figures 16, 18, 20 and 17, 19, 21 show flow fields of turbulence intensity of steel flow in the zone of argon injection through porous plug no. 1 and 2, respectively. The turbulence intensity is expressed by the following formula:

$$I = \frac{\sqrt{\frac{2}{3}k}}{u} \tag{19}$$

where: u – mean velocity of fluid [m/s], k – kinetic energy of turbulence [m^2/s^2].

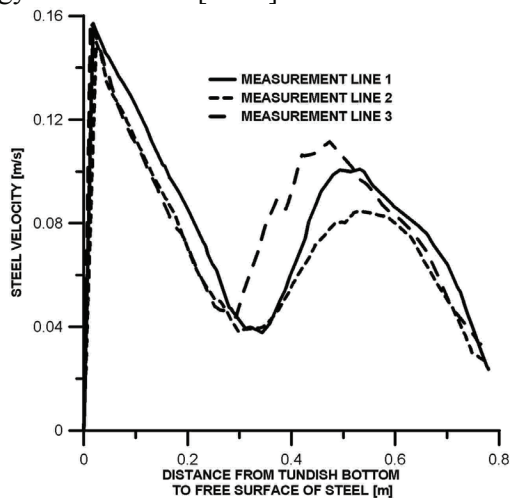

Fig. 11. Steel velocity along measurement line in the zone of Ar injection through blow shape number 2 (shape factor of bubble = 0.8)

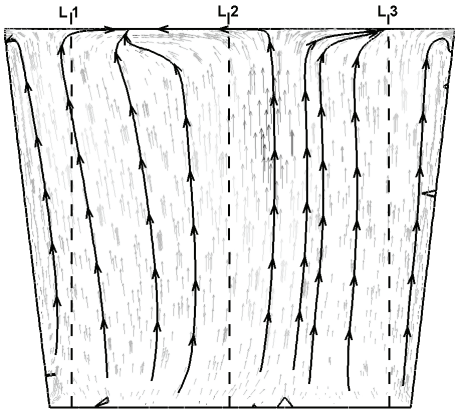

Fig. 12. Steel flow in the zone of Ar injection through blow shape number 1 (shape factor of bubble = 0.6)

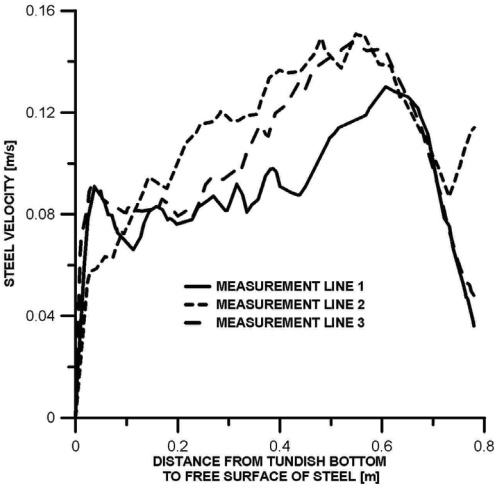

Fig. 13. Steel velocity along measurement line in the zone of Ar injection through blow shape number 1 (shape factor of bubble = 0.6)

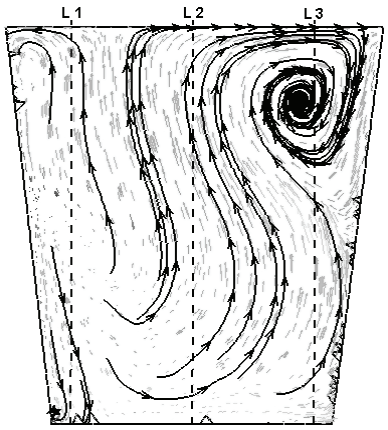

Fig. 14. Steel flow in the zone of Ar injection through blow shape number 2 (shape factor of bubble = 0.6)

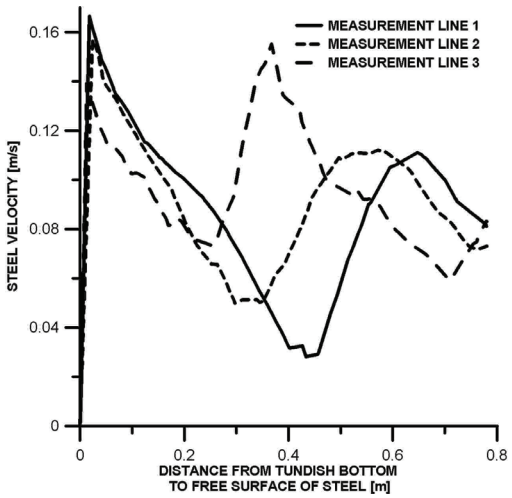

Fig. 15. Steel velocity along measurement line in the zone of Ar injection through blow shape number 2 (shape factor of bubble = 0.6)

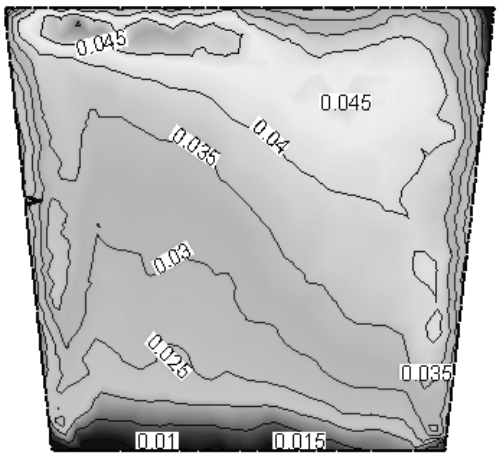

Fig. 16. Distribution of turbulence intensity in the zone of Ar injection through blow shape number 1 (spherical shape of bubble)

The turbulence intensity accepts value from 0 to 1. Figures 16-21 display asymmetrical distribution of turbulence intensity. The bubbles determine by shape factor generate higher values of turbulence intensity in analysed zones of argon injection.

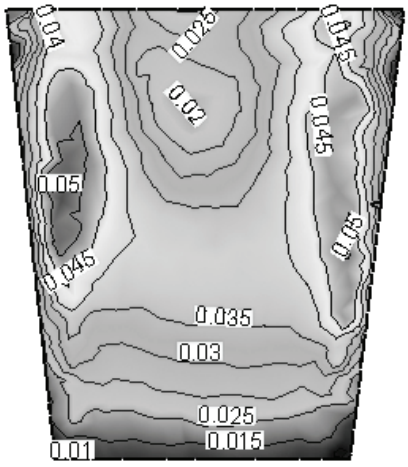

Fig. 17. Distribution of turbulence intensity in the zone of Ar injection through blow shape number 2 (spherical shape of bubble)

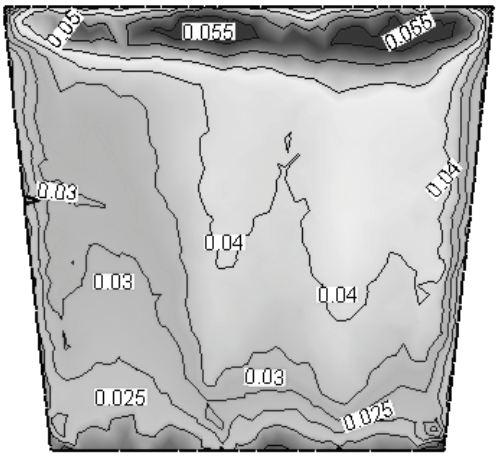

Fig. 18. Distribution of turbulence intensity in the zone of Ar injection through blow shape number 1 (shape factor of bubble = 0.8)

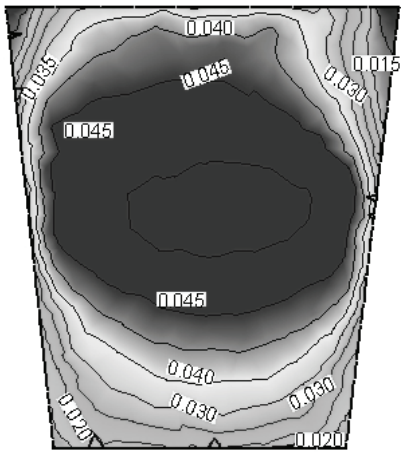

Fig. 19. Distribution of turbulence intensity in the zone of Ar injection through blow shape number 2 (shape factor of bubble = 0.8)

The results obtained for particular variants of computation of steel velocity field and turbulence intensity field in the argon injection zones indicate a potential for change in the hydrodynamic charac-

teristics of the facility. Therefore, in order to make a comprehensive assessment of steel flow through the tundish for the computation variants under consideration, RTD curves and the shares of individual flow zones were additionally determined. Using the relationships provided in the work of (Sahai and Emi 1996, Mazumdar and Guthrie 1999), the percentage shares of stagnant, plug and ideal-mixing flows were determined, respectively. The considered types of flow are characterized in the work of (Jowsa at al. 2005). The use of devices controlling the flow of steel in the tundish is aimed at minimizing the share of stagnant flow and increasing the plug flow share, while inducing the desirable orientation of steel flow within the tundish. Figures 22 to 24 show RTD curves for the computation variants under analysis, by recorded variations in marker concentration in particular tundish outlets. The RTD curve distributions presented in the figures show that the curves for individual outlets are similar to one another,

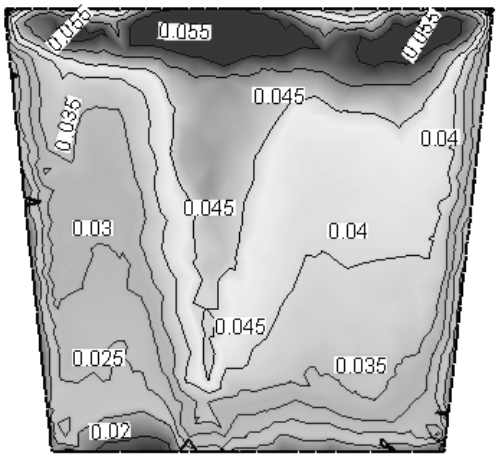

Fig. 20. Distribution of turbulence intensity in the zone of Ar injection through blow shape number 1 (shape factor of bubble = 0.6)

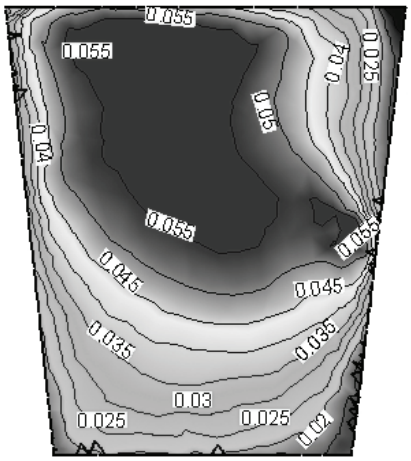

Fig. 21. Distribution of turbulence intensity in the zone of Ar injection through blow shape number 2 (shape factor of bubble = 0.6)

which indicates little effect of the modification of the injected bubble shape on the macroscopic picture of steel flow in the tundish. The calculated average percentage shares of particular flows confirm this fact, as shown in Table 1. The obtained results for particular shapes of bubbles blown in by the injection system differ by 2% for the case of both stagnant, plug and ideal-mixing flow.

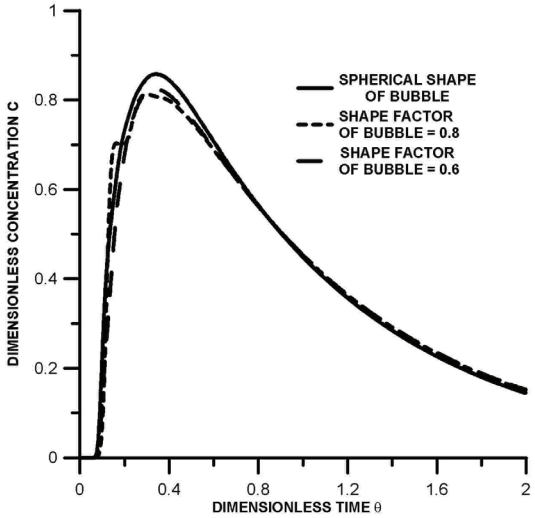

Fig. 22. Residence time distribution curve for the tundish outlet number 1

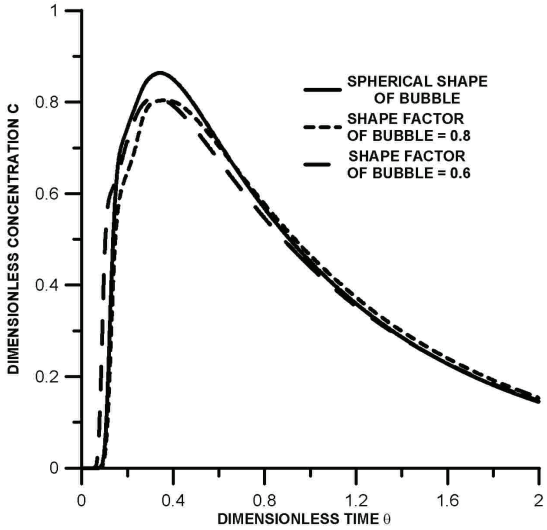

Fig. 23. Residence time distribution curve for the tundish outlet number 2

Table 1. Steel flow characteristic in consider tundishes

Type of gaseous bubble	Average participation [%]		
	Volume of stagnant flow	Volume of plug flow	Volume of ideal mixing flow
Spherical bubble	34,1	12,3	53,5
Shape factor of bubble = 0.8	35,6	11,5	52,8
Shape factor of bubble = 0.6	36,2	12,1	51,6

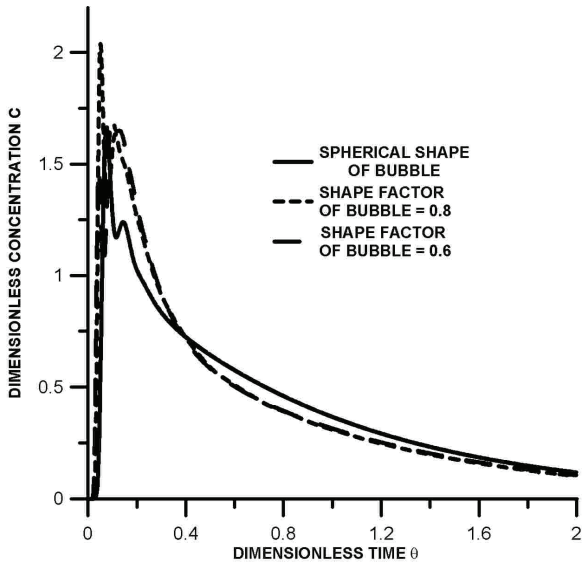

Fig. 24. Residence time distribution curve for the tundish outlet number 3

4. SUMMARY

The phenomena associated with the flow of gas bubbles through the liquid steel are complex enough to continue to be the subject of research. The application of argon in steel metallurgy is accompanied not only by studies aimed at explaining the phenomena occurring between the gas, metal, slag and solid (e.g. solid non-metallic inclusion) phases, but also those that are involved with the development of new argon application technologies and the improvement of already developed ones. The application of some simplifying assumptions (idealizations) in the mathematical model arouses the doubt about whether this does not lead to a significant distortion of simulation results, as it is the case for gas bubbles taking on a spherical shape. In the case of argon injection to the liquid steel in the tundish, the obtained results made it possible to dissipate this doubt. The computation results concerning the direction of motion and velocity of steel, the turbulence intensity of steel flow, the shape of RTD curves and the volumes of particular flows, presented in this article, indicate that the assumption of a non-spherical bubble shape will not have any significant effect on the macroscopic hydrodynamic conditions prevailing in the tundish. This is so, because so important and sensitive characteristics as the RTD curves and the individual flow volumes differ insignificantly.

ACKNOWLEDGEMENTS

This work has been financed within the BW-2-204/202/2002/P Project.

REFERENCES

Anagbo, P.E., Brimacombe, J.K., 1990, Plume Characteristics and Liquid Circulation in Gas Injection through a Porous Plug, *Metall. Mater. Trans. B*, 21B, 637-648.

Anioła-Kusiak, A., Lux, A., Mamro, K., Rzeszowski, M., 1981, Metalurgia argonowa stali, *Biblioteka Metalurga, Wyd. Śląsk*. (in Polish).

Cwudziński, A., Jowsa, J., 2006, Charakterystyki RTD przepływu stali w kadzi pośredniej z podstrumieniowym regulatorem turbulencji i systemem iniekcji argonu, *Hutnik – Wiadomości Hutnicze,* 73, 538-541 (in Polish).

Guy, M., de Poloni, I., Blostein, P., Devaux, M., 1991, Argon Bubbling in the Tundish Aciers D'allevard, *1st European Conf. on Continuous Casting*, 193-202

Haider, A., Levenspiel, O., 1989, Drag Coefficient and Terminal Velocity of Spherical and Nonspherical Particles, *Powder Technology,* 58, 63-70.

Iguchi, M., Nozawa, K., Tomida, H., Morita, Z-I., 1992a, Bubble Characteristics in the BuoyancyRegion of a Vertical Bubbling Jet, *ISIJ Int.,* 32, 747-754.

Iguchi, M., Morita, Z.-I., Tokunaga, H., Tatemichi, H., 1992b, Bubble Expansion Due to Heat Transfer during Gas Injection, *6th Int. Con. on Refining Processes,* Lulea, 113-128.

Iguchi, M., Kawabata, H., Nakajima, K., Morita, Z.-I., 1995, Measurement of Bubble Characteristics in Molten Iron Bath at 1600°C Using Electroresistivity Probe, *Metall. Mater. Trans. B*, 26B, 67-74.

Iguchi, M., Nakatani, T., Tokunaga, H., 1997, The Shape of Bubble Rising near the Nozzle Exit in Molten Metal Baths, *Metall. Mater. Trans. B*, 28B, 417-423.

Jowsa, J., Merder, T., Bogusławski, A., Mendrek, A., 2005, Charakterystyki mieszania podczas odlewania stali przy użyciu sześciowylewowej kadzi pośredniej, *Hutnik – Wiadomości Hutnicze,* 72, 377-383 (in Polish).

Mazumdar, D., Guthrie, R.I.L., 1999, The Physical and Mathematical Modelling of Continuous Casting Tundish Systems, *ISIJ Int.*, 39, 524-547

Morales, R.D., Ramos-Banderas, A., Sanchez-Perez, R., 2004, Mathematical Simulation and Modeling of Steel Flow with Gas Bubbling in Trough Type Tundish, *AISTech Proceedings,* Vol. II, 867-877.

Moravec, R., Valek, L., 2004, Veryfication of Blowing Conditions of Inert Gas in Tundish CCM, *Acta Metallurgica Slovaca,* Vol. 3, 394-399.

Moravec, R., Valek, L., Pys, J., 2005, Physical Modeling of Argon Bubbling, *1st Int. Conf. Simulation and Modelling of Metallurgical Processes in Steelmaking*, 107-114.

Pieprzyca, J., Kudliński, Z., Lipiński, J., 2006, Rola przedmuchiwania stali gazami obojętnymi w kadzi pośredniej na podstawie fizycznych badań modelowych, *Polska Metalurgia w latach 2002-2006*, 191-196 (in Polish).

Rzeszowski, M., Zieliński, K., Ptasińska, J., Mendak, D., 2003, Wpływ osłony strumienia metalu i budowy kadzi pośredniej na czystość metalurgiczną i jakość wyrobów gotowych, *Hutnik – Wiadomości Hutnicze,* 70, 60-65 (in Polish).

Sahai, Y., Emi, T., 1996, Melt Flow Characterization in Continuous Casting Tundishes, *ISIJ Int.*, 36, 667-672

Sheng, Y.Y., Irons, G.A., 1995, The Impact of Bubble Dynamics on the Flow in Plumes of Ladle Water Models, *Metall. Mater. Trans. B*, 26B, 625-635.

Stolte, G., 2002, Secondary Metallurgy, *Verlag Stahleisen GmbH*.

Szekely, J., Themelis, N.J., 1971, Rate Phenomena in Process Metallurgy, *John Wiley & Sons, Inc*.

Tatsuoka, T., Kamata, C., Ito, K., 1997, Expansion of Injected Gas Bubble and its Effects on Bath Mixing under Reduced Pressure, *ISIJ Int.,* 37, 557-561.

Zhou, M., Brimacombe, J.K., 1994, Critical Fluid Flow Phenomena in a Gas-Stirred Ladle, *Metall. Mater. Trans. B*, 25B, 681-693.

Yokoya, S., Takagi, S., Iguchi, M., Marukawa, K., Hara, S., 2000, Formation of Fine Bubble through Swirling Motion of Liquid Metal in the Metallurgical Container, *ISIJ Int.,* 40, 572-577.

MODELOWANIE NUMERYCZNE WPŁYWU WSPÓŁCZYNNIKA KSZTAŁTU PĘCHERZA GAZOWEGO NA PRZEPŁYW STALI W KADZI POŚREDNIEJ Z SYSTEMEM INIEKCJI ARGONU

Streszczenie

Artykuł przedstawia wyniki symulacji komputerowej przepływu stali w sześciootworowej kadzi pośredniej wyposażonej w podstrumieniowy regulator turbulencji i system iniekcji argonu. Autorzy wykorzystali technikę modelowania numerycznego CFD (Computational Fluid Dynamics) dla pokazania wpływu różnych wariantów kształtu pęcherza gazowego (pęcherze kuliste i nie kuliste) na ruch stali w strefie wdmuchiwania gazu i kształt krzywych RTD (Residence Time Distribution). Symulacje były wykonane dla warunków izotermicznych. W efekcie obliczeń otrzymano pola przepływu stali, pola intensywności turbulencji, krzywe RTD oraz udziały procentowe poszczególnych stref przepływu (przepływ stagnacyjny, tłokowy i idealnego mieszania).

Submitted: August 28, 2007
Submitted in a revised form: February 5, 2008
Accepted: April 14, 2008